Authentic Microgrid State Estimation

Fei Feng , Graduate Student Member, IEEE, Peng Zhang, Senior Member, IEEE, and Yifan Zhou, Member, IEEE

Abstract—An error-resilient state estimation is devised to calculate authentic states for microgrids equipped with hierarchical controls. New contributions include: 1) a state estimation incorporating droop control which helps mitigate estimation errors due to transient disturbance; 2) a secondary-control-empowered microgrid state estimation for leveraging power sharing and voltage regulation among DERs. Case studies demonstrate the robustness, efficiency and excellent convergence performance of the authentic state estimation approach.

Index Terms—State estimation, microgrid, droop control, secondary control.

I. INTRODUCTION

ICROGRID is a promising paradigm for hosting distributed energy resources (DERs) and improving electricity resiliency [1]. Reliable operations of microgrids depend on situational awareness and accurate power flow observations [2], which in turn rely on accurate state estimation (SE) to provide high quality initial inputs [3].

Today's microgrids unexceptionally adopt hierarchical power sharing and voltage control schemes to enable stable and autonomous islanded operations. Existing state estimation approaches based on traditional power flow formulations, however, fail to represent the physics of microgrids. The main reason is that none of the DERs equipped with droop and secondary controllers should be modeled as a swing bus which balances power mismatch [2]. Recently, a decentralized approach is developed to estate the states in a distribution network integrated with microgrids [4]. A state estimation for hybrid ac/dc microgrids is established in [5] where Lagrangian multipliers are used to decompose the microgrid subsystems and to distributionally solve the state estimation problem. In those existing algorithms, microgrids are modeled in the same way as traditional distribution feeders where a main grid or an infinite source supports the downstream system. Failing to represent droop/secondary regulation in DERs renders state estimation unable to find true microgrid states. When a microgrid is subject to unforeseeable

Manuscript received June 29, 2021; revised October 30, 2021; accepted January 1, 2022. Date of publication January 14, 2022; date of current version March 28, 2022. This work was supported in part by the National Science Foundation under Grants ECCS-2018492 and OIA-2040599. Paper no. PESL-00153-2021. (Corresponding author: Peng Zhang)

The authors are with the Department of Electrical and Computer Engineering, Stony Brook University, Stony Brook, NY 11794-2350 USA (e-mail: fei.feng@stonybrook.edu; p.zhang@stonybrook.edu; yi-fan.zhou.1@stonybrook.edu).

Color versions of one or more figures in this article are available at https://doi.org/10.1109/TPWRS.2022.3143362.

Digital Object Identifier 10.1109/TPWRS.2022.3143362

disturbances, traditional state estimation can provide erroneous results, which jeopardize its usefulness in microgrid energy management and operations.

To tackle the challenges, this letter devises an authentic microgrid state estimation (AMSE) approach which effectively offsets evaluation errors that otherwise would be significant. By fully incorporating droop/secondary control functionalities, AMSE creates an accurate replica of microgrids states and is resilient to exogenous disturbances or false data injections.

II. AUTHENTIC MICROGRID STATE ESTIMATION

A. Droop-Incorporated AMSE

Weighted least square is adopted to minimize the squared errors of state measurements. For a microgrid equipped with hierarical control, a new cost function is devised as follows:

$$\boldsymbol{J}(\boldsymbol{\theta}, \boldsymbol{V}, f) = \left[\boldsymbol{z} - \boldsymbol{h}(\boldsymbol{\theta}, \boldsymbol{V}, f)\right]^{T} \boldsymbol{R}^{-1} \left[\boldsymbol{z} - \boldsymbol{h}(\boldsymbol{\theta}, \boldsymbol{V}, f)\right]$$
(1)

where θ and $V \in \mathbb{R}^{N \times 1}$ are angles and magnitudes of bus voltages, respectively, z is the measurement vector, R is the error variance matrix. Here $h(\theta, V, f)$ is the function mapping the measurements to the electrical variables and is detailed as:

$$h(\theta, V, f) = \begin{bmatrix} S(V, \theta) \\ S_{kl}(V, \theta) \\ V \\ f \end{bmatrix} = \begin{bmatrix} \bar{Y}(\theta) \cdot V \circ V \\ \bar{Y}(\theta) \circ V_k \circ V_l \\ V \\ f \end{bmatrix}$$
(2)

where $S(V, \theta) = [P(V, \theta), Q(V, \theta)]^T$ is the power injection vector; $S_{kl}(V, \theta) = [P_{kl}(V, \theta), Q_{kl}(V, \theta)]^T$ is a vector of branch flow from bus k to bus l; and \circ denotes Hadamard product. Different from traditional state estimation, frequency f is considered as a variable coupled with the outputs of DERs. $\bar{Y}(\theta)$ is the extended admittance matrix of microgrid, defined

$$\bar{\boldsymbol{Y}}(\boldsymbol{\theta}) = \begin{bmatrix} \boldsymbol{Y}_p(\boldsymbol{\theta}) \\ \boldsymbol{Y}_q(\boldsymbol{\theta}) \end{bmatrix} = \begin{bmatrix} |Y_{kl}| \cos(\theta_k - \theta_l - \delta_{kl}) \\ |Y_{kl}| \sin(\theta_k - \theta_l - \delta_{kl}) \end{bmatrix}$$
(3)

where $|Y_{kl}|$ and δ_{kl} are the admittance magnitude and angle of branch k-l. The new formula can be iteratively updated to achieve the minimal cost function as follows:

$$\mathbf{H}^{T}\mathbf{R}^{-1}(\mathbf{z} - \mathbf{h}(\mathbf{x})) = (\mathbf{H}^{T}\mathbf{R}^{-1}\mathbf{H})\Delta\mathbf{x}$$
(4)

where, $x = [\theta, V, f]^T$ is set to simply the scale, H is the Jacobian matrix of the measurement h(x).

0885-8950 © 2022 IEEE. Personal use is permitted, but republication/redistribution requires IEEE permission. See https://www.ieee.org/publications/rights/index.html for more information.

In the steady state, the active/reactive power sharing among DERs can be incorporated into power injections of DERs by droop logics as follows:

$$S(V, \theta, f) = \begin{bmatrix} Y_p(\theta) \cdot V \circ V + m_G \circ (f - f^{ref}) \\ Y_q(\theta) \cdot V \circ V + n_G \circ (V - V^{ref}) \end{bmatrix}$$
(5)

where, m_G and n_G are the reciprocal of droop coefficients vectors, respectively; f^{ref} is the frequency reference; and V^{ref} is the voltage reference vector.

Once H and h(x) are evaluated at the end of each iteration, the microgrid variables θ , V, f can be updated for the next iteration by (4). The AMSE iterations continue until the errors in those variables reaches the tolerance ξ . See Algorithm 1 for the AMSE pseudo code.

B. AMSE Scheme Empowered With Secondary Control

Secondary control aims to achieve power sharing and voltage recovery. Real power increments can be adjusted among DERs. To be specific, a secondary control variable is added to assist frequency recovery. Then, the secondary control effect can be integrated into real power injections from DERs, as follows:

$$P(V, \theta, f) = \left[Y_p(\theta) \cdot V \circ V + m_G \circ (f - f^{ref^*}) \right] \quad (6)$$

where, $f^{ref^*} = f^{ref} + \Omega$ is a desired frequency reference containing the integral of the local frequency error Ω .

The adjustment of the DERs' reactive power estimation depends on secondary control schemes, exemplified using three representative schemes as follows:

1) Power Sharing Mode (PS): The PS scheme aims to shift DERs' droop-based curves to achieve proportional power sharing. The adjustment of reactive power can be devised as follows:

$$Q(V, \theta) = \left[Y_q(\theta) \cdot V \circ V - \gamma \cdot Q_G^* \right]$$
 (7)

where Q_G^* indicates the rated values of DERs' power injections, the sharing ratio $\gamma = Q_{G,l}/Q_{G,l}^*$, $Q_{G,l}$ and $Q_{G,l}^*$ are the droop-based reactive power output and rated value of the leader DER, respectively.

2) Voltage Regulation Mode (VR): The target of VR is to fully recover the DER bus voltages back to their rated values. In steady state, we integrate a dummy bus to regulate the var injections from the DER buses, which can be expressed as:

$$Q(V, \theta)$$

$$= [\boldsymbol{Y}_q(\boldsymbol{\theta}) \cdot \boldsymbol{V} \circ \boldsymbol{V} - diag(\boldsymbol{V}) \boldsymbol{Y}_d(\boldsymbol{V}_a + \boldsymbol{V}^* - 2\boldsymbol{V})] \quad (8)$$

Here, dummy bus voltages V_a are defined as $V_a = V_a^p + V^* - V$, where V_a^p are the dummy bus voltages at the previous iteration, and V^* denotes the rated voltages. When a DER bus' estimated voltage is lower than its rated value, a positive deviation will be superimposed to the dummy bus voltage to adjust the DERs' reactive power output based on (8). The opposite will be performed when the DER bus voltage is higher than the rated value. Such a negative feedback process, if convergent, will recover DER bus voltages to rated values. We insert a virtual admittance matrix Y_d between each dummy bus and its corresponding DER bus, which not only convert voltage to reactive power but also can adjust convergence rate.

```
Algorithm 1: AMSE Algorithm.
```

```
Initialize: z, \theta, V, f, \xi, Y_d, R;

Update: z (PS/VR/ST) Eq. (2-4);

while \Delta \theta, \Delta f, \Delta V, \Delta \gamma (PS/ST), \Delta V_a(VR/ST) \geq \xi do

if DER bus then

| Update: H, h(x) Eq. (5-8);

else

| Update: H, h(x)Eq. (2);

end

Update: \theta, V, f;

end

Result: \theta, V, f.
```

TABLE I
MEAN SQUARED ERRORS OF AMSE AND CSE UNDER DISTURBANCES

σ	Droop	PS	VR	ST	
	AMSE/CSE	AMSE/CSE	AMSE/CSE	AMSE/CSE	
0.01	2.38e-5/0.0037	1.42e-5/0.0031	1.79e-7/0.0041	3.20e-6/0.0034	
0.02	5.21e-5/0.0120	6.64e-5/0.0145	2.77e-7/0.0123	4.54e-6/0.0118	
0.03	1.17e-4/0.0290	1.49e-4/0.0285	4.32e-7/0.0316	6.07e-6/0.0309	
0.04	2.13e-4/0.0442	2.53e-4/0.0455	6.23e-7/0.0591	8.65e-6/0.0487	
0.05	2.45e-4/0.0672	3.55e-4/0.0843	1.05e-6/0.0752	1.01e-5/0.0854	

3) Smart Tuning Mode (ST): One DER bus in outer loop implements the VR mode while others adopt the PS mode [6].

Without loss of generality, the aforementioned AMSE framework is discussed in the context of AC microgrids. Nevertheless, the principle of AMSE is generic and equally applicable for DC microgrids where hierarchical P/V control schemes are adopted.

III. CASE STUDY

The effectiveness and efficiency of AMSE are verified on a 33-bus system with 5 DERs [6]. The P/f and Q/V droop coefficients of the DER buses 1, 6, 13, 25 and 33 are respectively selected as $m_G = n_G = [0.05, 1, 0.1, 1, 0.2]^T$. Virtual admittance Y_d for VR mode is unity. All the algorithms are implemented in MAT-LAB 2018a on a 2.50 GHz PC. The following measurements are taken for state estimation implementations: 1) active/reactive flows through all lines; 2) active/reactive power injections at those buses with loads; 3) frequency of the system; 4) voltages at selected buses.

A. Validity of AMSE

This subsection verifies the effectiveness of AMSE by comparing AMSE results against those from classical Gauss Newton method (CSE) [7].

1) Robustness Against Disturbances: We first validate the robustness of AMSE against disturbances. It is assumed that injected disturbances follow Gauss distribution with $N(\mu,\sigma^2)$. Fig. 1 presents the distributions of bus voltages obtained from AMSE and CSE under different controls (i.e., droop, PS, VR, and ST modes). Specifically, for each control mode, 100 cases are randomly generated with disturbances sampled from $N(0.01,0.01^2)$. AMSE and CSE are conducted using those disturbed measurements. Table I further presents the mean squared

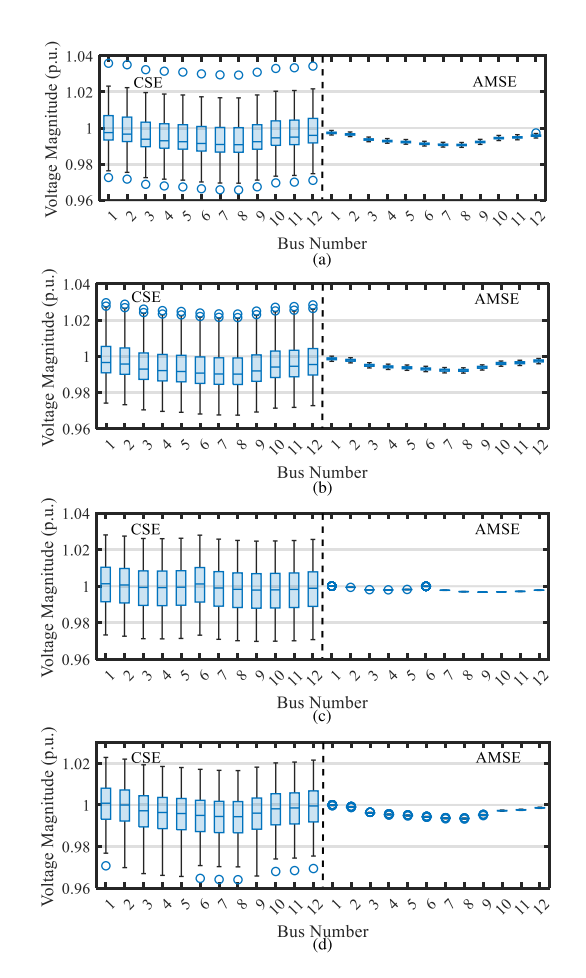


Fig. 1. Voltage distributions of AMSE v.s. CSE with disturbances under different controls, (a) Droop, (b) PS, (c) VR, (d) ST.

errors of AMSE and CSE under different disturbance levels. Following observations can be obtained:

- 1) The droop-based AMSE outperforms CSE in terms of the robustness against disturbances. For instance, in Fig. 1(a), the voltage distributions of AMSE under the disturbance of $N(0.01,0.01^2)$ are much narrower than those of CSE. This is because CSE relies on a swing bus to balance the disturbances. Rather, AMSE reassigns the disturbance into multiple DERs which desensitize the droop-based microgrid state estimation to disturbed data. Figs. 1(b)-(d) show the secondary-based AMSE methods (e.g. PS, VR and ST) are robust against disturbances as well.
- 2) Table I further validates the accuracy and robustness of both droop-based and secondary-based AMSE under different scales of disturbances. For instance, with the disturbances N(0.01,0.01²), the error of droop-based AMSE (2.38e-5) is much lower than that of CSE (0.0037). Meanwhile, CSE results deteriorate with the growth of disturbance substantially. Nonetheless, those of AMSE are slightly increased.
- 2) Robustness Against Bad Data Injections: Next, we demonstrate AMSE's robustness against bad data injections. It is assumed that the measurements of power injections at buses 4, 5, and 9 are maliciously modified by $\pm 10\%$. Simulation

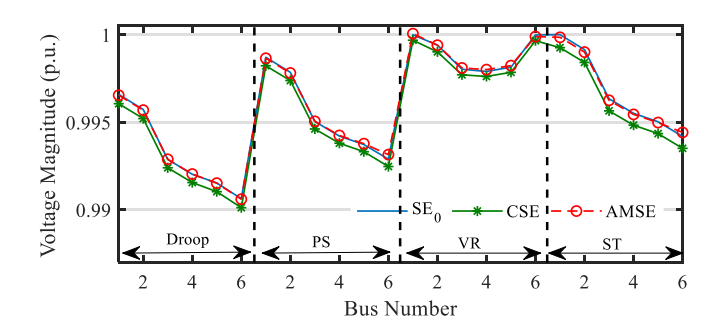


Fig. 2. Voltage estimation results under bad data injections.

TABLE II
MEAN SQUARED ERRORS OF AMSE AND CSE UNDER BAD DATA INJECTIONS

Droop	PS	VR	ST	
AMSE/CSE	AMSE/CSE	AMSE/CSE	AMSE/CSE	
5.26e-8/2.35e-6	1.45e-6/1.02e-5	4.12e-8/8.37e-6		

TABLE III
CONVERGENCE AND COMPUTING TIME OF AMSE V.S. CSE

σ	-	Droop AMSE/CSE	PS AMSE/CSEE	VR AMSE/CSE	ST AMSE/CSE
0.01	Iter. T/s	8/4 0.0467/0.0298	8/4 0.0525/0.0329	8/4 0.0618/0.0320	11/4 0.0739/0.0257
0.05	Iter. T/s	8/4 0.0458/0.0292	8/6 0.0519/0.0407	8/5 0.0683/0.0334	11/4 0.0695/0.0289

results are provided in Fig. 2 and Table II. Fig. 2 illustrates partial voltages of AMSE and CSE under different controls with the presence of bad data injections. It can be observed that AMSE relieves state estimation errors when bad data exist in the measurement. For example, compared with CSE, the voltages of AMSE under different modes are closer to SE₀ which is state estimation results without noise and bad data. Further, Table II presents the mean squared errors of AMSE and CSE. Simulation shows that under all control modes, the accuracy of AMSE is consistently improved compared with that of CSE, which validates the robustness of AMSE against bad data effects.

B. AMSE Convergence Performance

Table III summarizes the convergence and computation performances of AMSE and CSE under different disturbances. It can be observed that:

- 1) The AMSE has similar convergence performances with those of CSE under different controls. For instance, the AMSE with $N(0.01,0.01^2)$ requires 8 iterations to reach the tolerance while CSE requires 4 iterations.
- 2) The convergence of AMSE is less affected by disturbances. For instance, as shown in Table III, the number of iteration of AMSE with $N(0.01,0.01^2)$ is 8 which is identical to that with $N(0.01,0.05^2)$. Meanwhile, the computation time of AMSE (about 0.05-0.07 s) is acceptable as well.

Specifically, the VR-based AMSE relies on Y_d to perform the iterative computation, as defined in (8). Therefore, Table IV

TABLE IV CONVERGENCE OF VR-AMSE WITH DIFFERENT $oldsymbol{Y}_d$ and Disturbances

Y_d	1000	333	200	125	100	33	20	10
$\sigma = 0.01$	8	11	19	38	46	156	301	622
$\sigma = 0.02$	8	11	19	38	46	156	301	622
$\sigma = 0.03$	8	11	19	38	46	162	311	624
$\sigma = 0.04$	8	11	19	38	46	165	311	625
$\sigma = 0.05$	8	11	19	38	46	170	320	629

investigates the convergence of VR-based AMSE under different \boldsymbol{Y}_d and disturbances.

- 1) The convergence performance of VR-AMSE is significantly impacted by \mathbf{Y}_d . For instance, the number of iteration under $\mathbf{Y}_d = 1000$ is 8, whereas 301 iterations are required under $\mathbf{Y}_d = 20$. This is because VR-AMSE with a larger \mathbf{Y}_d will take more aggressive reactions to the difference of voltages at each iteration.
- 2) Meanwhile, the convergence of VR-AMSE with larger \boldsymbol{Y}_d is more robust against disturbances. For example, given a disturbance of $N(0.01,0.01^2)$, the number of iteration of AMSE is 301 under $\boldsymbol{Y}_d=20$. When the disturbance is as large as $N(0.01,0.05^2)$, the iteration number reaches 320.

IV. CONCLUSION

We devise an authentic state estimation algorithm which incorporates hierarchical control effects and tolerates disturbances or false injections in data. Case studies validate the effectiveness of the new state estimation method under different disturbance levels and various control modes.

REFERENCES

- P. Zhang, Networked Microgrids. Cambridge, U.K.: Cambridge Univ. Press, 2021.
- [2] F. Feng and P. Zhang, "Implicit Z_{bus} Gauss algorithm revisited," *IEEE Trans. Power Syst.*, vol. 35, no. 5, pp. 4108–4111, Sep. 2020.
- [3] J. Zhao *et al.*, "Roles of dynamic state estimation in power system modeling, monitoring and operation," *IEEE Trans. Power Syst.*, vol. 36, no. 3, pp. 2462–2472, May 2020.
- [4] C. Lin, W. Wu, and Y. Guo, "Decentralized robust state estimation of active distribution grids incorporating microgrids based on PMU measurements," *IEEE Trans. Smart Grid*, vol. 11, no. 1, pp. 810–820, Jan. 2020.
- [5] N. Xia, H. B. Gooi, S. Chen, and W. Hu, "Decentralized state estimation for hybrid AC/DC microgrids," *IEEE Syst. J.*, vol. 12, no. 1, pp. 434–443, Mar. 2018.
- [6] F. Feng and P. Zhang, "Enhanced microgrid power flow incorporating hierarchical control," *IEEE Trans. Power Syst.*, vol. 35, no. 3, pp. 2463–2466, May 2020.
- [7] A. Monticelli, State Estimation in Electric Power Systems: A Generalized Approach. New York, NY, USA: Springer, 2012.